Published in final edited form as:
IEEE Trans Ultrason Ferroelectr Freq Control. 2008 December ; 55(12): 2714–2718. doi:10.1109/TUFFC.2008.987.

Characterization of a 40-MHz Focused Transducer with a Fiber Grating Laser Hydrophone

Sien-Ting Lau,
Department of Applied Physics and Materials Research Centre, The Hong Kong Polytechnic University, Hung Hom, Kowloon, Hong Kong SAR, China (email: apstlau@polyu.edu.hk)

Li-Yang Shao,
Photonics Research Centre, Department of Electrical Engineering, The Hong Kong Polytechnic University, Hung Hom, Kowloon, Hong Kong SAR, China

Helen Lai-Wa Chan,
Department of Applied Physics and Materials Research Centre, The Hong Kong Polytechnic University, Hung Hom, Kowloon, Hong Kong SAR, China (email: apstlau@polyu.edu.hk)

Hwa-Yaw Tam,
Photonics Research Centre, Department of Electrical Engineering, The Hong Kong Polytechnic University, Hung Hom, Kowloon, Hong Kong SAR, China

Chang-Hong Hu,
Department of Biomedical Engineering, University of Southern California, Los Angeles, CA

Hyung-Ham Kim,
Department of Biomedical Engineering, University of Southern California, Los Angeles, CA

Ruibin Liu,
Department of Biomedical Engineering, University of Southern California, Los Angeles, CA

Qifa Zhou, and
Department of Biomedical Engineering, University of Southern California, Los Angeles, CA

K. Kirk Shung
Department of Biomedical Engineering, University of Southern California, Los Angeles, CA

Abstract

A novel fiber-optic hydrophone based on a dual-polarization, short-cavity fiber grating laser as the sensing element is described. Wet chemical etching was used to fabricate a thinned fiber sensor to extend its frequency response as well as spatial resolution. The lateral beam profile at the focal plane of a 40-MHz lens-focused lithium niobate ($LiNbO_3$) transducer was measured with the fiber sensor, and a tomographic technique was used to compute the transducer profile, which is compared with that obtained by a PVDF hydrophone. The fiber hydrophone has a sensitivity of approximately −259 dB re 1V/μPa up to 40 MHz, which is higher than that of a commercial PVDF hydrophone. Moreover, it is capable of accurately characterizing the beam generated by high-frequency transducer.

I. INTRODUCTION

Ultrasound is frequently used in clinical imaging and has become indispensable in the disciplines of cardiology, obstetrics, and gynecology. Medical imaging at frequencies higher than 20 M Hz has become very important in clinical applications that require high resolution [1], [2]. For characterizing such ultrasonic equipment and assessing the safety of patient

exposure, considerable effort has been put into developing high-performance ultrasonic hydrophones.

Conventional PVDF or P(VDF-TrFE) hydrophones have been widely used in medical ultrasound for measuring output from ultrasonic imaging/ therapeutic equipment [3], [4]. These hydrophones provide good sensitivity as their acoustic impedances are close to the load medium (i.e., water and human tissues). However, when the ultrasound frequency is increased, the size of the hydrophone needs to be decreased. With the sensing element smaller than a fraction of 1 mm, the sensitivity diminishes significantly. The electrical impedance matching and cable shunting also become problematic and a specially designed buffer amplifier has to be placed adjacent to the tiny sensing element. Recently, fiber-optic hydrophones have been explored as alternatives for the detection of ultrasound. Fiber-optic sensors have many advantages over conventional hydrophones, including immunity from electromagnetic interference, intrinsic safety, small size, light weight, and capacity to multiplex with negligible cross-talk between the sensors. Fiber-optic hydrophones based on interferometric and polarimetric approaches [5]–[8], as well as fiber Bragg grating [9], [10], have been reported by others.

We have demonstrated and patented [11] a novel fiber-optic hydrophone with a dual polarization distributed Bragg reflector (DBR) fiber laser as the sensing element [12], [13]. The detection principle of the fiber-optic hydrophone is based on the modulation of the birefringence of the laser cavity by acoustic pressure. Consequently, the beat frequency of the 2 orthogonal polarization modes of the fiber grating laser is induced in response to the high-frequency ultrasound. It should be capable of measuring high-frequency ultrasound up to several tens of megahertz. This technique greatly simplifies signal extraction, avoiding the use of the unbalanced interferometer and phase modulator required in hydrophones based on pseudoheterodyning fiber grating lasers [10], [14].

In this paper, we report the use of a wet etching technique to reduce the diameter of a dual polarization DBR fiber laser to enhance its spatial resolution and extend its frequency response. The beam profile measurement of a high-frequency focused transducer is made with this thinned fiber sensor, and a tomographic reconstruction of the acoustic field in a plane perpendicular to the beam is performed. The result is compared with that obtained by a PVDF hydrophone.

II. THEORY

A. Operating Principle of the Fiber Grating Laser Sensor

The operating principle of the proposed fiber grating laser hydrophone is based on the anisotropic index changes (i.e., birefringence) induced by acoustic pressure. Fig. 1 shows the basic configuration of a fiber grating laser. The diameter of the phosphosilicate Er/Yb core is 4.66 μm and the B-Ge-Si photosensitive annulus has an outside diameter of approximately 16 μm. Two fiber Bragg gratings (FBGs) with identical reflection wavelengths of ~1550 nm are written in the photosensitive fiber to create an in-fiber cavity. The fiber grating laser operates over 2 orthogonal polarization modes because of the fiber birefringence introduced during fiber fabrication and grating inscription. For a low birefringent fiber ($n_s \approx n_f \approx n$, where $n_{s,f}$ are the modal refractive indexes), the beat frequency can be expressed as

$$\Delta\nu = \frac{B\nu}{n} \tag{1}$$

where ν is the lasing frequency and $B = n_s - n_f$ is the induced birefringence. A polarizer is used to align these 2 polarization modes in the same state and the polarization beat frequency Δν of the laser can be generated. The beating signal is directed to a photodetector and measured with a commercial RF-spectrum analyzer.

When the laser cavity is subjected to an acoustic field, its refractive index is changed due to the photoelastic effect of the fiber. For an acoustic wavelength comparable with or much smaller than the fiber diameter, the acoustic pressure induces refractive index change along and perpendicular to the direction of the acoustic wave, thus changing the fiber birefringence. The induced change in birefringence is given by [7]:

$$\Delta B = \mathrm{kp} \sin \omega t \cos 2\theta \tag{2}$$

where k is a constant depending on the acoustic frequency and the photoelastic coefficients and refractive index of the fiber; p and ω are the amplitude and angular frequency of the acoustic pressure, respectively; and θ is the angle between the slow axis of the fiber and the propagation direction of the acoustic wave. Hence, the frequency modulation of the beat carrier produced by fiber laser is the result. By measuring the frequency shifts and amplitudes of the upper and lower sideband frequency components of the laser output with a high-speed photodetector and RF-spectrum analyzer, the frequency and amplitude of the acoustic signal can be determined. In most practical situations, the acoustic pressure along the fiber sensor is not uniform. Provided that the fiber is parallel to the acoustic wavefront (i.e., the line of constant phase), the induced beat frequency change is given by

$$\delta\Delta\nu = \Delta\nu \frac{k \int_0^L \mathrm{pdl}}{\mathrm{BL}} \sin \omega t \cos 2\theta \tag{3}$$

where L is the length of the laser cavity. Therefore, the laser output of the sensor is the line integral of the acoustic pressure amplitude across the laser cavity.

B. Tomographic Reconstruction

For the beam profile measurement, the fiber is scanned across the ultrasonic beam in a plane normal to the beam axis, and a parallel projection $P_\phi(D)$ at a given angle is obtained (as shown in Fig. 2) along the axis D described by the expression $D = x \cos \phi + y \sin \phi$. The measured projection $P_\phi(D)$ is formed by combining a set of line integrals of acoustic pressure along the length of the laser cavity. Provided that the laser cavity is long enough to intercept the whole beam, the tomographic reconstruction of the pressure profile $P(x, y)$ is performed using the filtered backprojection algorithm [15] with the Shepp-Logan filter. The measured projection $P_{\phi i}(D)$ is first filtered. The filtered projection $Q_{\phi i}(D)$ is obtained by:

$$Q_{\phi i}(n\tau) = \tau \times \mathrm{IFFT}\left\{\mathrm{FFT}\left\{P_{\phi i}(n\tau)\right\} \times \mathrm{FFT}\{h(n\tau)\}\right\} \tag{4}$$

where τ is the sampling interval of the projections, and

$$h(n\tau) = \frac{-2}{\pi(4n^2 - 1)} \tag{5}$$

is the Shepp-Logan filter, which is actually the convolution of Ram-Lak filter [16] with sinc function. The Shepp-Logan filter is chosen to reduce the noise because of the roll-off at higher

frequency. The reconstructed pressure profile is obtained by the backprojection of the filtered projections:

$$P(x,y)=\sum_{i=1}^{N_p} Q_{\phi i}(x\cos\phi i + y\sin\phi i) \tag{6}$$

where N_p is the number of projections uniformly distributed over 180°.

III. EXPERIMENTS

A. Fabrication of Thinned Fiber Sensor

A pair of 1551-nm Bragg gratings with a separation of 17.5 mm was written in a Er/Yb co-doped fiber to construct the DBR fiber laser. The length of one grating was 10 mm with a reflectivity over 99%; the other one was 3 mm long with a reflectivity of around 90%. To enhance the spatial resolution of the fiber sensor, thinning of the fiber cladding layer was achieved by wet chemical etching. The DBR fiber laser was fixed on a Teflon frame and then immersed in a 24% hydrofluoric acid HF solution. The acid bath was kept at constant temperature of 30°C, allowing an etching rate of ~1 μm/min. The fiber would become difficult to handle if too much of the cladding layer was etched away; in this case the diameter of the fiber laser was reduced to ~63 μm.

B. Sensitivity and Beam Profile Measurement

A schematic diagram of the experimental setup is shown in Fig. 3. Photographs of the fiber and PVDF hydrophone are shown in Fig. 4. Both the transducer and the fiber laser sensor were placed in a tank filled with distilled and degassed water. The transducer was a single-element 40-MHz $LiNbO_3$ device [17] incorporating a lens for focusing and 2 matching layers for acoustic matching. It had an aperture size of 3 mm and a focal length of 9 mm. The transducer was driven at its center frequency to generate an ultrasonic wave.

The fiber laser sensor was excited by pumping with a 980-nm semiconductor laser via a 980/1550 wavelength-division-multiplexer (WDM). 1550-nm laser light was emitted from both ends of the fiber laser. Most of the out-put was emitted from the 3-mm FBG end and directed to the 1550-nm port of the WDM. An optical isolator (ISO) was placed in front of the photodetector to reduce any unwanted reflection back to the fiber laser. The beat signal was generated using a polarizer to align the 2 polarization modes in the same state and directed to the photodetector (PD). According to (2), the maximum ΔB value can be achieved at $\theta = 0$ or 90°, suggesting that either of the polarization axes of the fiber should be aligned in the propagation direction of the acoustic wave. Rotation of the fiber about its axis was made to maintain the maximum sensitivity throughout the experiment. An RF-spectrum analyzer connected to the PD was used to record the received signal S of the fiber sensor, expressed in dBm (relative to P_o = 1 mW), which can be converted into voltage by:

$$V_f=\sqrt{\mathrm{RP}_o\left(10^{S/10}\right)} \tag{7}$$

where R is the input impedance of the spectrum analyzer (= 50 Ω).

To determine the sensitivity of the fiber hydrophone, a needle-type PVDF hydrophone (element size of 40 μm, Precision Acoustics Ltd., Dorchester, UK) with known sensitivity was used to

measure the acoustic pressure p at the same testing distance. The sensitivity of the fiber hydrophone was calculated by:

$$M = \frac{V_f}{p} \tag{8}$$

where M is expressed in terms of dB relative to 1 V/μPa.

For the beam profile measurement, the fiber sensor was also positioned at the focal point of the transducer. The lateral beam profile of the transducer was then measured by scanning the fiber sensor at a 10-μm step across the ultrasonic beam in the plane perpendicular to the beam propagation direction (X-Z plane as shown in Fig. 3). For comparison, the PVDF hydrophone was also used to measure the transducer beam profile.

IV. RESULTS AND DISCUSSIONS

The beat signal spectra of the fiber laser sensor recorded by the spectrum analyzer are shown in Fig. 5. It can be seen that a beat signal (at f = 1.02 GHz) with a carrier-to-noise ratio of about −70 dB was recorded when the fiber laser was pumped by a 980-nm semiconductor laser with the power of about 46 mW (Fig. 5a). The out-put power of the DBR fiber laser was 2.5 mW. During the measurement, the fiber was subjected to the ultrasound generated by the focused transducer in continuous mode, with both the upper and lower sidebands observed (Fig. 5b). The sensitivity of the fiber hydrophone was determined by a comparison method in which the received signal [converted into voltage by (7)] was compared with that of the PVDF hydrophone with known sensitivity, with the result shown in Fig. 6. The frequency response of the fiber hydrophone varied within ±2 dB in the frequency range of 35 to 42 M Hz. In comparison with the PVDF hydrophone, the fiber hydrophone showed higher sensitivity.

By scanning the fiber hydrophone across the ultrasonic beam generated by the transducer, the parallel projection profile was obtained (Fig. 7). In this work, the transducer was rotated 6° per step over a span of 180°, thus making 30 projections measured with the fiber sensor. The reconstruction of the ultrasound pressure field was then performed using the filtered back-projection algorithm with the Shepp-Logan filter. For comparison, a PVDF hydrophone was also used in characterizing the lateral beam profile. The peak pressure at the focus of the transducer was found to be 2.3 M Pa when the transducer is excited by a Panametrics pulser/receiver Model 5900PR at a 1 μJ setting. Fig. 8 shows the reconstructed pressure profile and the corresponding profile obtained by the PVDF hydrophone. It can be seen that the 3-dB beam width (at the normalized amplitude decreased to 0.71) measured by both the fiber and PVDF hydrophones match fairly well, indicating that this fiber sensor is capable of measuring the beam profile of a high-frequency transducer.

V. CONCLUSIONS

A thinned fiber-optic acoustic pressure sensor that employed a dual polarization short-cavity fiber laser has been demonstrated. Based on the modulation of the birefringence of the in-fiber laser by acoustic pressure, the sensor is capable of detecting ultrasound up to a frequency of 42 M Hz with good sensitivity (approximate −259 dB re 1V/μPa). With its small diameter (~63 μm), the fiber-optic sensor can be used for accurate characterization of narrow beam width generated by highly focused transducers or transducer arrays used in medical imaging.

Acknowledgments

This work was supported by the Centre for Smart Materials (CSM) of the Hong Kong Polytechnic University and the Hong Kong Research Grants Council (Project No. PolyU 5198/03E) and NIH Grant P41-EB002182.

REFERENCES

1. Foster FS, Ryan LK, Turnbull DH. Characterization of lead zirconate titanate ceramics for use in miniature high-frequency (20–80 MHz) transducers. IEEE Trans. Ultrason., Ferroelect., Freq. Contr 1991;vol. 38(no 5):446–453.
2. Zipparo MJ, Shung KK, Shrout TR. Piezoceramics for high-frequency (20 to 100 MHz) single-element imaging transducers. IEEE Trans. Ultrason., Ferroelect., Freq. Contr 1997;vol. 44(no 5):1038–1048.
3. Harris GR. Hydrophone measurements in diagnostic ultrasound fields. IEEE Trans. Ultrason., Ferroelect., Freq. Contr 1988;vol. 35(no 2):87–101.
4. Lum P, Greenstein M, Grossman C, Szabo TL. High-frequency membrane hydrophone. IEEE Trans. Ultrason., Ferroelect., Freq. Contr 1996;vol. 43(no 4):536–544.
5. Beard PC, Mills TN. Miniature optical fibre ultrasonic hydrophone using a Fabry-Perot polymer film interferometer. Electron. Lett 1997;vol. 33:801–803.
6. Koch C. Measurement of ultrasonic pressure by heterodyne interferometry with a fiber-tip sensor. Appl. Opt 1999;vol. 38(no 13):2812–2819. [PubMed: 18319859]
7. Chan HLW, Chiang KS, Price DC, Gardner JL. The characterization of high-frequency ultrasonic fields using a polarimetric optical fiber sensor. J. Appl. Phys 1989;vol. 66:1565–1570.
8. Lewin PA, Mu C, Umchid S, Daryoush A, El-sherif M. Acousto-optic, point receiver hydrophone probe for operation up to 100 MHz. Ultrasonics 2005;vol. 43(no 10):815–821. [PubMed: 16054665]
9. Takahashi N, Yoshimura K, Takahashi S, Imamura K. Development of an optical fiber hydrophone with fiber Bragg grating. Ultrasonics 2000 Mar;vol. 38:581–585. [PubMed: 10829730]
10. Fisher NE, Surowiec J, Webb DJ, Jackson DA, Gavrilov LR, Hand JW, Zhang L, Bennion I. Ultrasonic hydrophone based on short in-fiber Bragg gratings. Appl. Opt 1998;vol. 37(no 34):8120–8128. [PubMed: 18301706]
11. Tam, HY.; Chan, HLW.; Guan, BO. Ultrasound sensor and ultrasound measurement device based on fibre laser sensor. U.S. Patent. 7 206 259. 2007 Apr.
12. Guan BO, Tam HY, Lau ST, Chan HLW. Ultrasonic hydrophone based on distributed Bragg reflection fiber laser. IEEE Photon. Technol. Lett 2005;vol. 16:169–171.
13. Lau ST, Liu SY, Tam HY, Chan HLW. Characterization of a fibre grating laser-based hydrophone for detection of high frequency medical ultrasound: a comparison with PVDF membrane hydrophone. Ferroelectrics 2006;vol. 333:115–120.
14. Lovseth SW, Kringlebotn JT, Ronnekleiv E, Blotekjaer K. Fiber distributed-feedback lasers used as acoustic sensors in air. Appl. Opt 1999;vol. 38(no 22):4821–4830. [PubMed: 18323971]
15. Kak, AC.; Slaney, M. Principles of Computerized Tomographic Imaging. New York: IEEE; 1987.
16. Horn BKP. Density reconstruction using arbitrary ray-sampling schemes. Proc. IEEE 1978 May;vol. 66(no 5):551–562.
17. Cannata JM, Zhao JZ, Ayyappan S, Ritter TA, Chen W, Shung KK. Fabrication of high frequency (25–75 MHz) single element ultrasonic transducers. Proc. IEEE Ultrasonic Symp 1999:1099–1103.

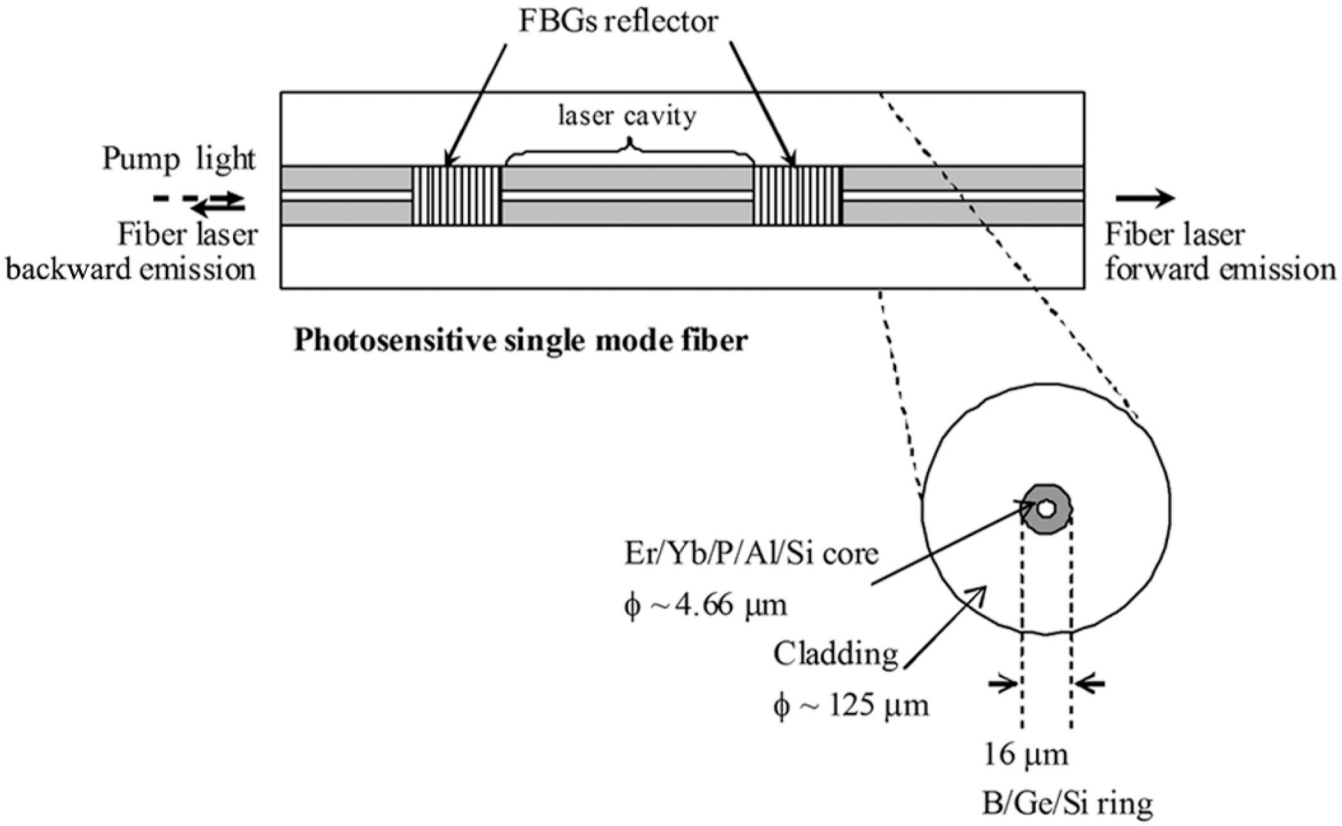

Fig. 1.
Fiber grating laser configuration.

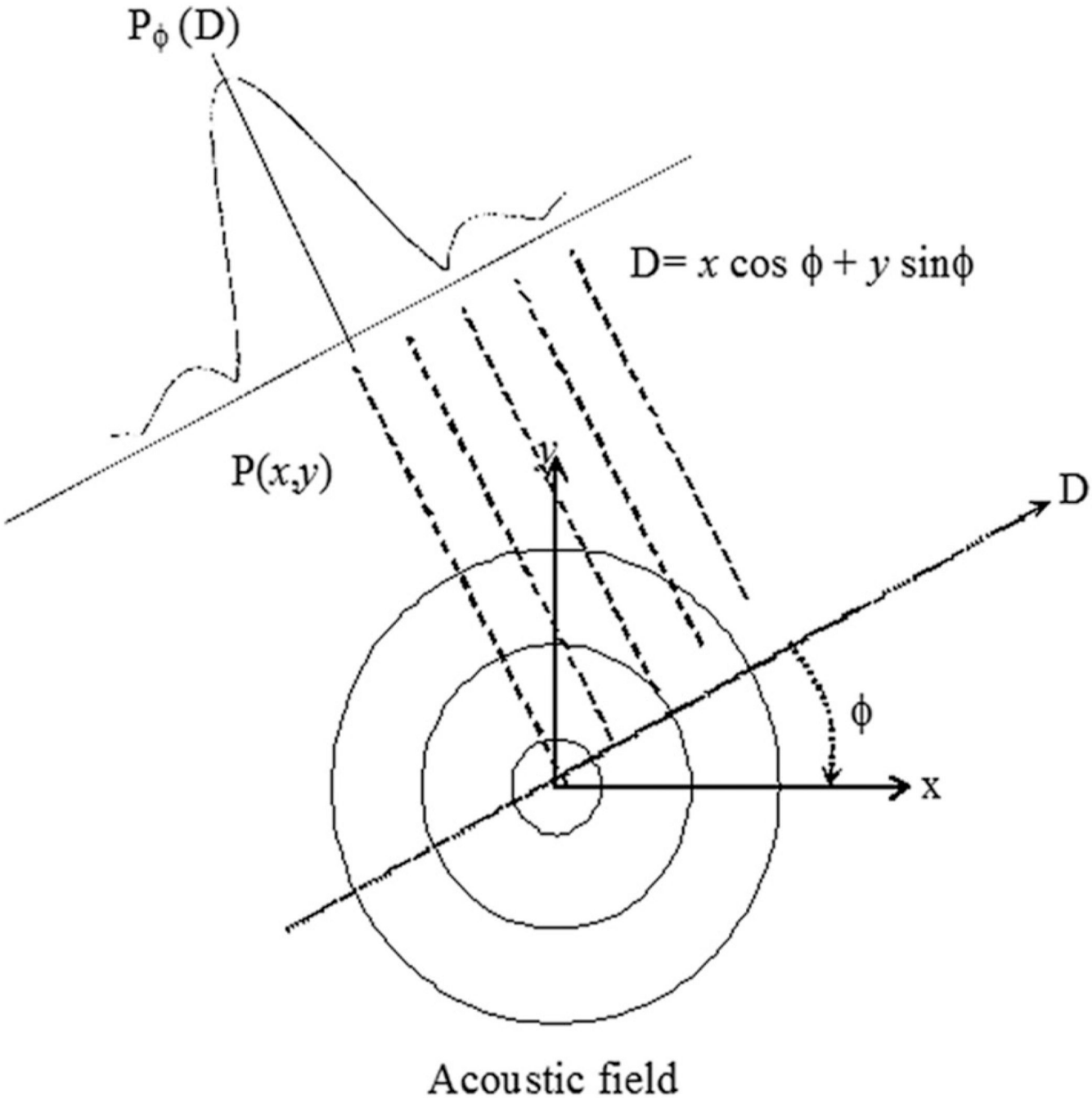

Fig. 2.
The pressure profile $P(x, y)$ and its parallel projection $P\phi(D)$ are shown for an angle ϕ.

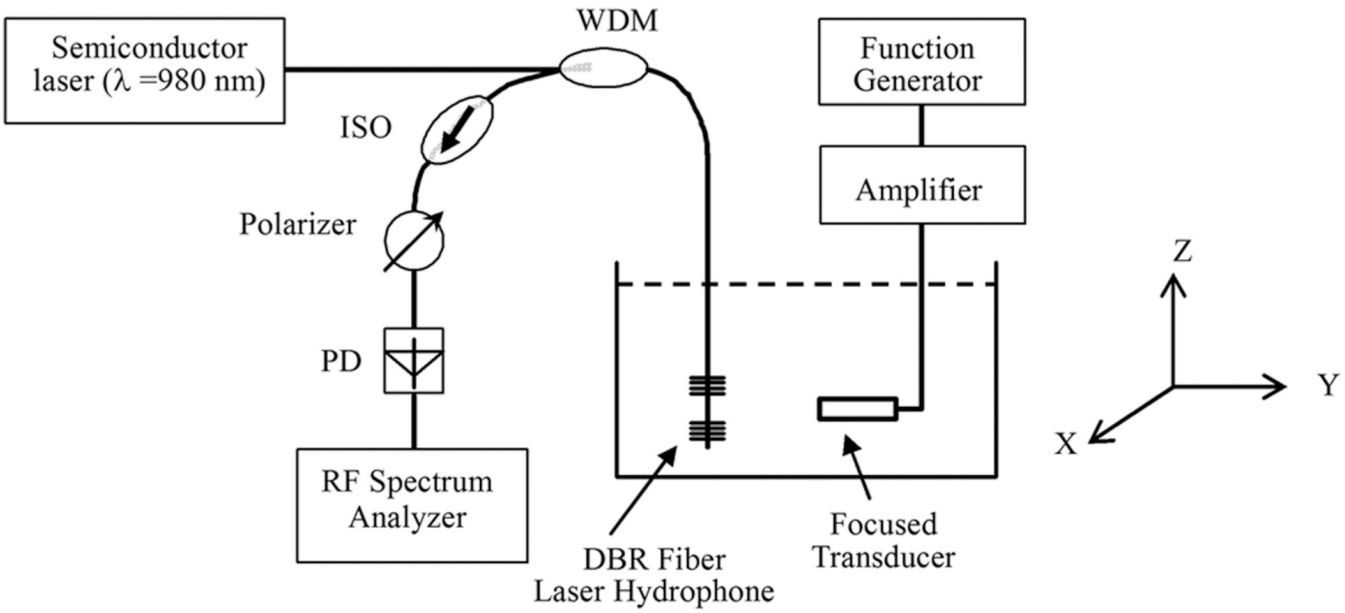

Fig. 3.
Schematic diagram of the experimental setup (ISO, isolator; PD, photodetector; WDM, wavelength division multiplexer).

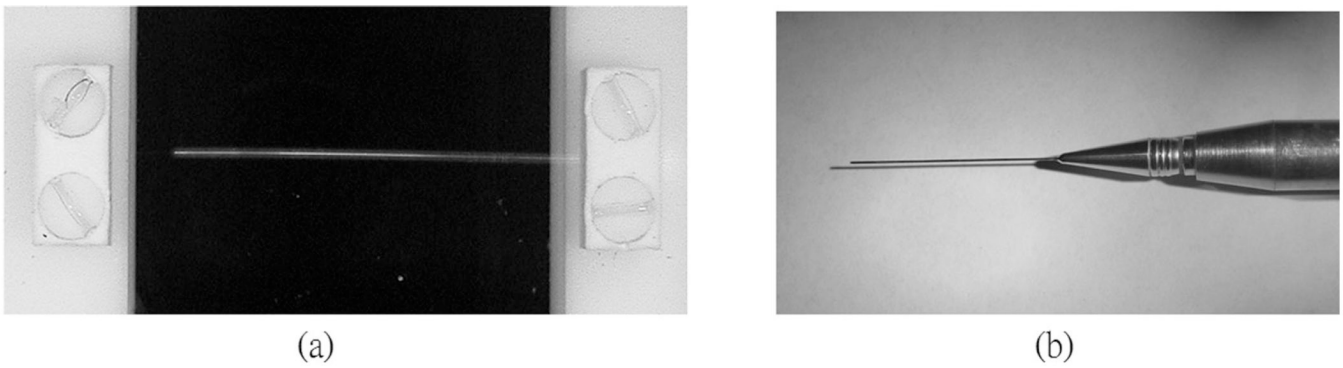

Fig. 4.
Photograph of the (a) fiber sensor and (b) PVDF hydrophone.

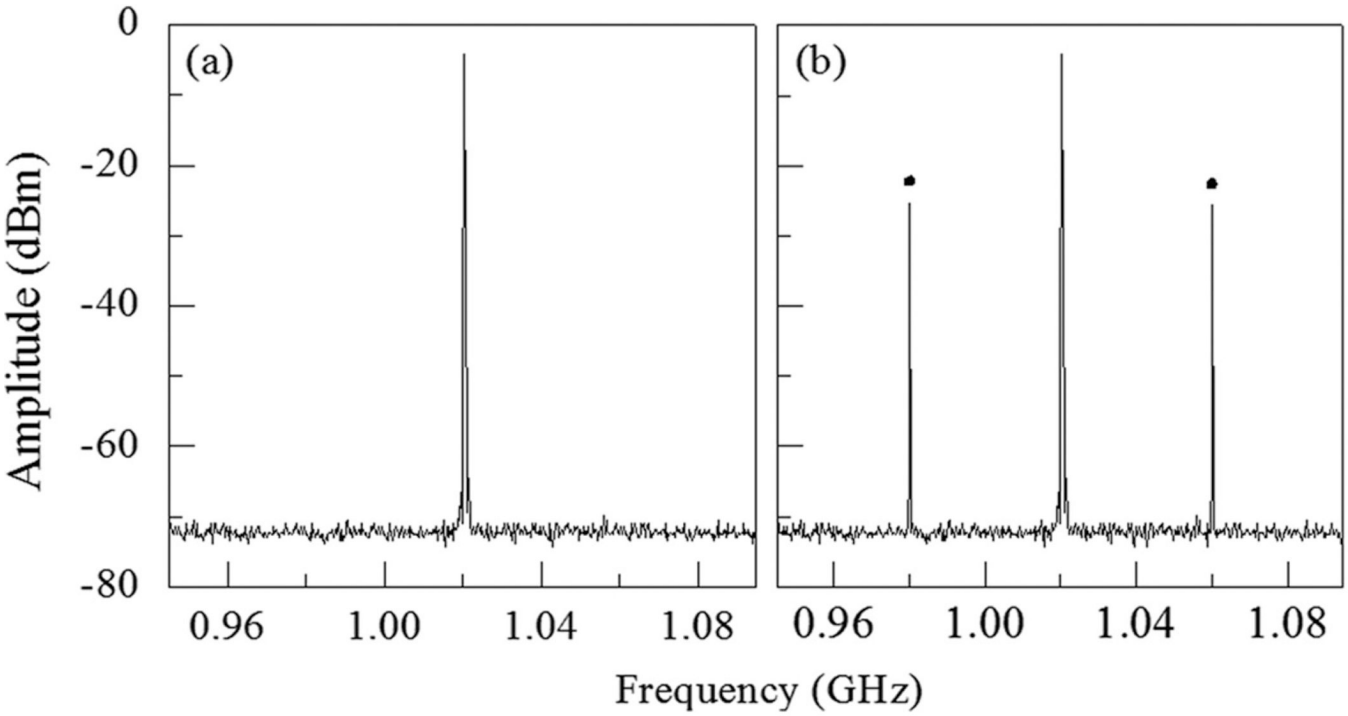

Fig. 5.

(a) Beat signal spectra of the DBR laser fiber sensor in response to the acoustic pressure generated by the focused transducer. (a) No (0 V) driving voltage; (b) 0.28 V driving voltage at 40 MHz.

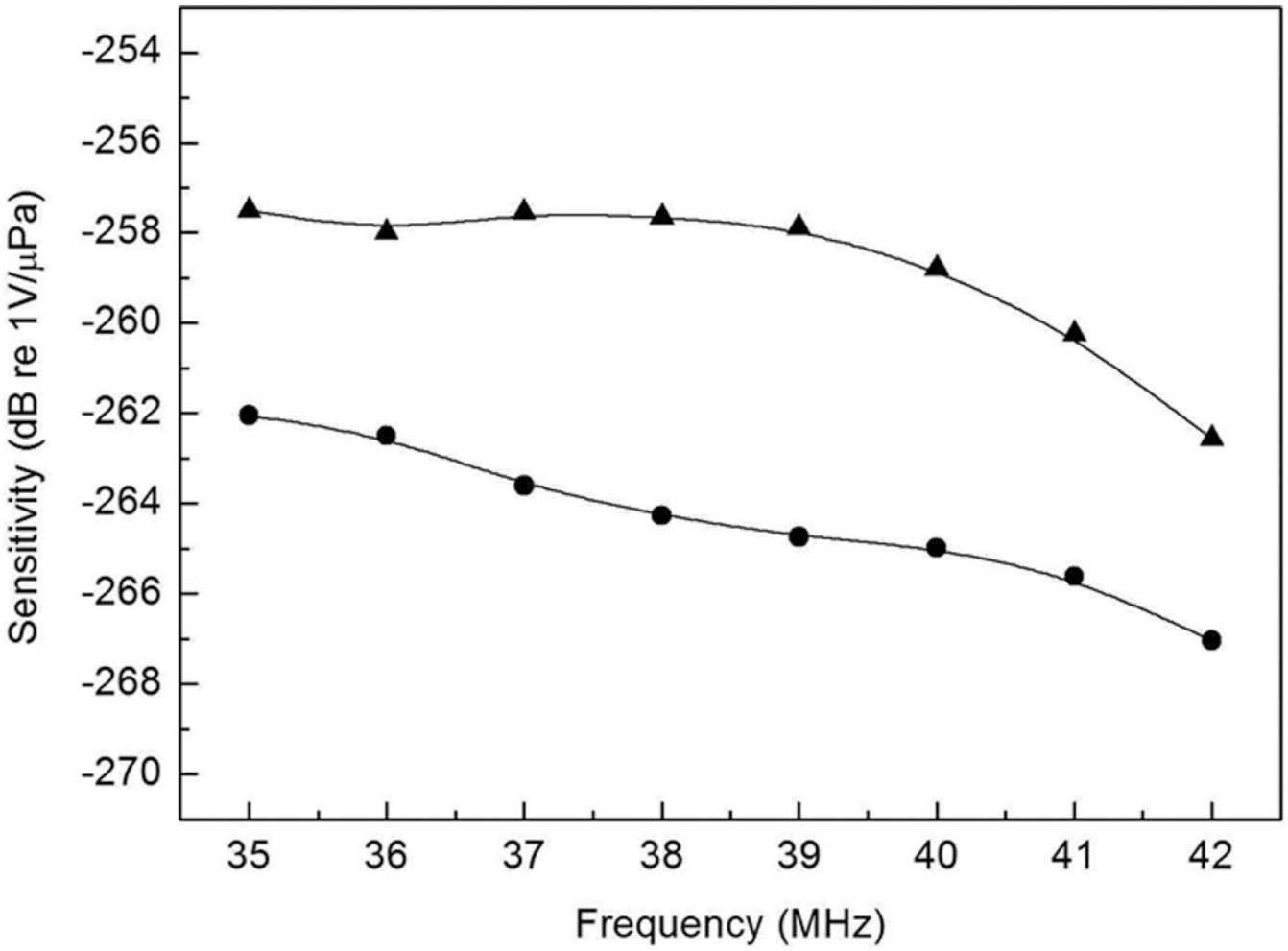

Fig. 6.
Frequency plot of the sensitivity of the fiber hydrophone (▲) and needle-type PVDF hydrophone (●).

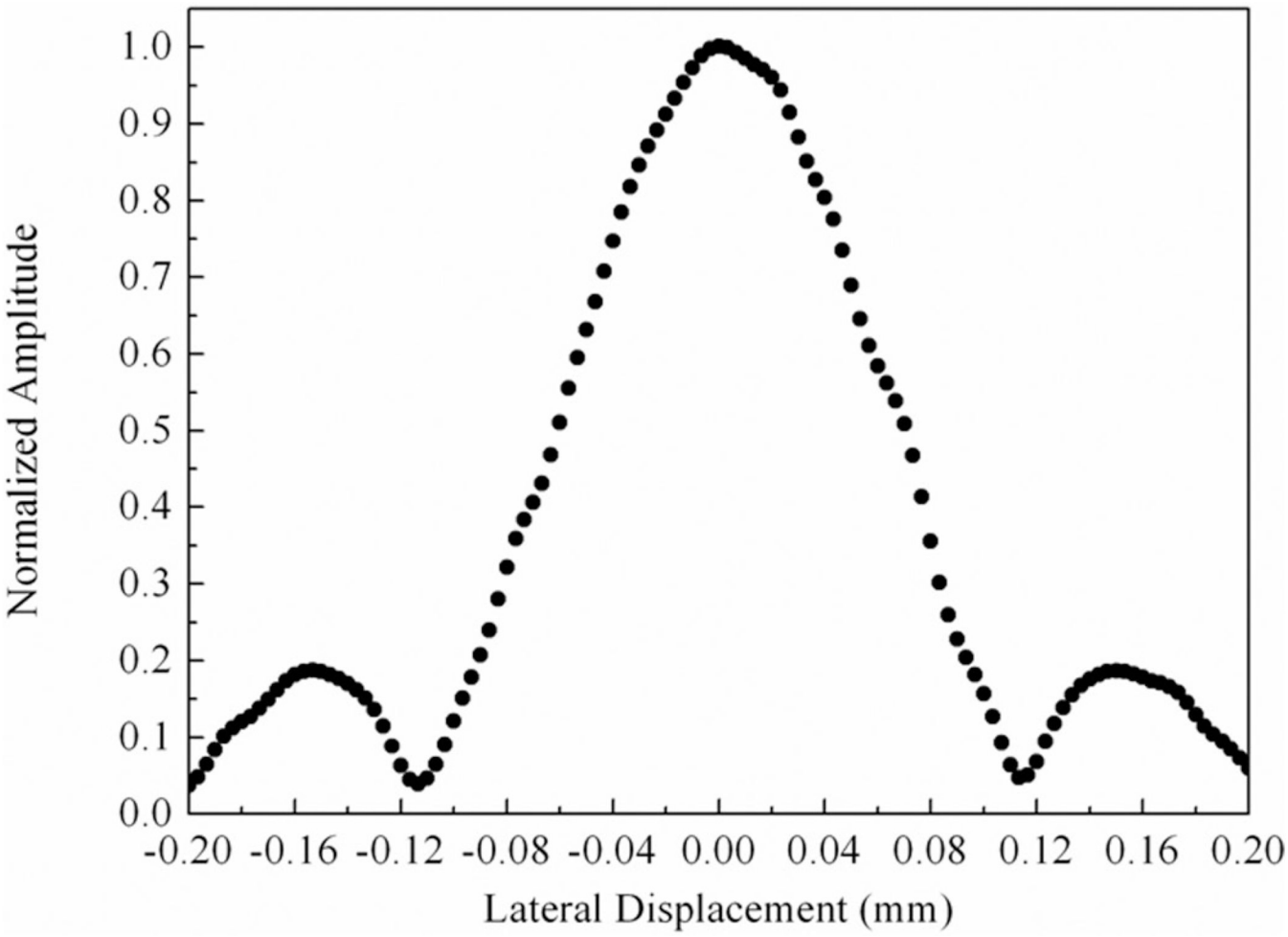

Fig. 7.
Normalized signal output from the DBR laser sensor as a function of the lateral displacement in a plane normal to the beam propagation direction.

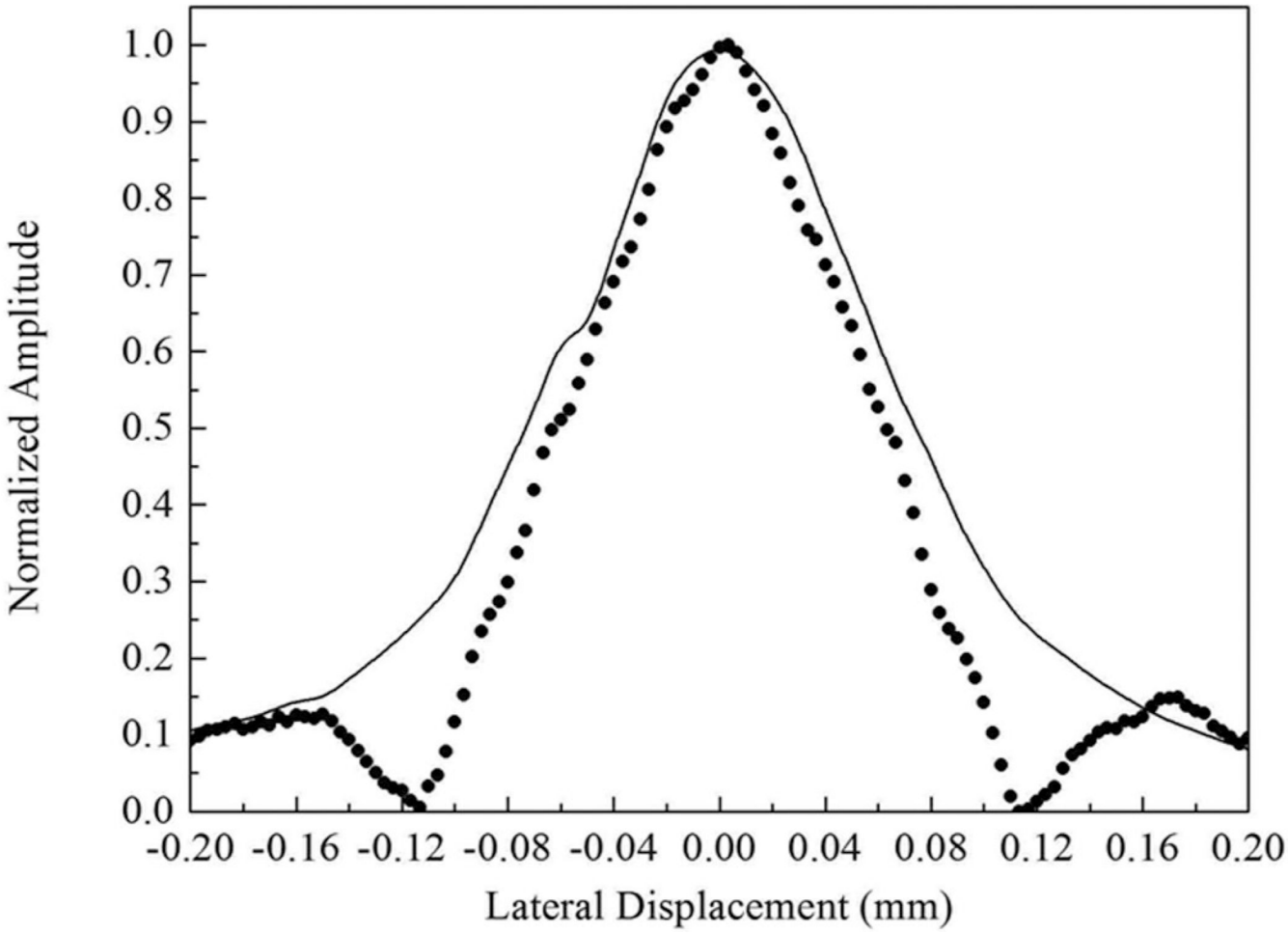

Fig. 8.

Normalized beam profile of the focused transducer in the focal plane. The symbol is the profile reconstructed from the fiber sensor data and the solid line is the profile obtained by using the PVDF hydrophone.